

Wave propagation of a functionally graded plate via integral variables with a hyperbolic arcsine function

Mokhtar Ellali¹, Mokhtar Bouazza^{2,4} and Ashraf M. Zenkour^{3,5}

1. *Smart structures Laboratory, University of Ain Temouchent, Ain Temouchent 46000, Algeria*

2. *Department of Civil Engineering, University Tahri Mohamed of Bechar, Bechar 08000, Algeria*

3. *Department of Mathematics, Faculty of Science, King Abdulaziz University, Jeddah 21589, Saudi Arabia*

4. *Laboratory of Materials and Hydrology (LMH), University of Sidi Bel Abbes, Sidi Bel Abbes 22000, Algeria*

5. *Department of Mathematics, Faculty of Science, Kafrelsheikh University, Kafrelsheikh 33516, Egypt*

Abstract: Several studies on functionally graded materials (FGMs) have been done by researchers, but few studies have dealt with the impact of the modification of the properties of materials with regard to the functional propagation of the waves in plates. This work aims to explore the effects of changing compositional characteristics and the volume fraction of the constituent of plate materials regarding the wave propagation response of thick plates of FGM. This model is based on a higher-order theory and a new displacement field with four unknowns that introduce indeterminate integral variables with a hyperbolic arcsine function. The FGM plate is assumed to consist of a mixture of metal and ceramic, and its properties change depending on the power functions of the thickness of the plate, such as linear, quadratic, cubic, and inverse quadratic. By utilizing Hamilton's principle, general formulae of the wave propagation were obtained to establish wave modes and phase velocity curves of the wave propagation in a functionally graded plate, including the effects of changing compositional characteristics of materials.

Keywords: FGM plate; effects of material properties; wave propagation; indeterminate integral variables; inverse sinus hyperbolic function

1 Introduction

The propagation of waves is a temporary local disturbance that moves in an elastic, homogeneous, and isotropic material medium without the transport of matter. A mechanical wave propagates with a transport of energy without the transport of matter. Wave propagation seems to have different applications (Zhang *et al.*, 2015; Ghorbanpour Arani *et al.*, 2017b; Hentati *et al.*, 2017). Recently, several studies of wave propagation in functionally graded material (FGM) constructions have been performed with the use of theoretical and numerical modeling. For example, Wang *et al.* (2010), analyzed the propagation of bending waves of nanoplates in an elastic foundation, based on the classical theory that utilizes initial stress. Aminipour *et al.* (2018) presented a new model for the analysis of wave propagation in anisotropic double-curvature

FGM shells. Aminipour and Janghorban (2017) used the trigonometric theory of shear strain for an analysis of wave propagation in anisotropic plates. Becheri *et al.* (2016) presented the theory of n -order shear strain plates to study the buckling of composites of simply supported symmetries with curvature effects.

Composites are used particularly in high technology applications. They also find applications in the field of civil engineering (Bouazza *et al.*, 2019a; Chen *et al.*, 2019; Gong *et al.*, 2021; Zeng *et al.*, 2023; Liang *et al.*, 2022; Bouazza and Zenkour, 2024). Ellali *et al.* (2018) investigated the buckling response of piezoelectric plates resting on the Pasternak foundation by applying the higher-order shear strain and analytical method. Bouazza *et al.* (2019b) presented a simple refined analytical theory of shear strain and numerical method that was offered by Ansys, in which in-plane and transverse displacements involve bending and shear components. The mechanical behavior of FGMs in a thermal environment using higher order shear deformation theories in which the material properties of FGMs are found by using different methods proved that the material is hot. Numerous other papers on the subject have been published, including Karami *et al.* (2018), Ghorbanpour Arani *et al.* (2020), Derbale *et al.* (2021), Merazka *et al.* (2021) and Ellali *et al.* (2022a).

Correspondence to: Mokhtar Bouazza, Department of Civil Engineering, University Tahri Mohamed of Bechar, Bechar 08000, Algeria
Tel.: +213-662462737
Email: bouazza_mokhtar@yahoo.fr;
bouazza.mokhtar@univ-bechar.dz

Received February 4, 2023; **Accepted** May 13, 2024

Naceri *et al.* (2011) examined the analysis of the propagation of single-walled carbon nanotubes (SWCNTs) and armchair sound waves in a thermal environment. Bouazza *et al.* (2016) analytically examined the thermal buckling of nano-plates resting on Winkler-Pasternak elastic foundations by using a non-local theory with four elasticity unknowns. Subsequently, Dihaj *et al.* (2018) used Euler Bernoulli's non-local theory to analyze the vibration of a chiral double-walled carbon nanotube in an elastic medium. Belmahi *et al.* (2018) examined the effect of boundary conditions on the vibration performance of a nanobeam of a polymer matrix material. Other papers have studied the behavior of FGM and sandwich plates, including Kouider *et al.* (2021), Liu *et al.* (2022), Hachemi *et al.* (2021), Bakoura *et al.* (2021), Bennedjadi *et al.* (2023), Bouazza and Zenkour (2018, 2020, 2021), Bouazza *et al.* (2018), Hadji *et al.* (2023), Bot *et al.* (2022), Al-Furjan *et al.* (2022a, 2022b, 2022c, 2023) and Chu *et al.* (2023). FGMs that have variable microstructures from one material to another, and the size of the microstructures involved ranges are typically of in several orders of magnitude; they can be modeled using classical continuum mechanics, but it also is possible that one can using non-continuum mechanics such as Li *et al.* (2015, 2016), Farrokhian (2020), Farrokhian and Salmani-Tehrani (2020), Keshtegar *et al.* (2020a, 2020b), Ghorbanpour Arani *et al.* (2016a, 2016b), Shahsavari *et al.* (2018, 2023), Guo *et al.* (2022), Kolahchi *et al.* (2020, 2022), Hajmohammad *et al.* (2018, 2021), and Wan *et al.* (2023).

Bouazza and Zenkour (2021) evaluated the impact of temperature and humidity on the vibration response of laminated composite plates by utilizing the refined four-variable n -order shear strain plate model. Sun and Luo (2011) explored wave propagation of FGM plates with simply supported supports, taking into account thermal impacts and temperature-dependent material properties by using the plate theory of order shear strain. New two-variable n th-form functions have been proposed by Bouazza *et al.* (2017). Tahir *et al.* (2021a) analyzed the wave propagation response of FGM plates with a hygrothermal effect, by employing different types of porosity. Ebrahimi and Seyfi (2022) analytically studied the wave propagation of foamed metal plates, including the Kerr substrate effect and the thermal environment. Qian *et al.* (2009) explored the transverse surface waves of structures that consisted of graduated functioning layers. Tahir *et al.* (2021b) presented an efficient theory of shear strain for FGM plates with different types of porosity variation in a viscoelastic foundation, based on a four-variable integral hyperbolic high order. Zhang *et al.* (2018) analytically studied the evanescent wave response of FGM-type spherical curved plates. Gafour *et al.* (2013) compared the structures of embedded zigzag double-walled carbon nanotubes (DWCNTs) to reality by studying the propagation of

sound waves in an elastic structure by employing the theory of nonlocal elasticity. Other interesting studies of dynamic problems and Wave propagation responses include Wang *et al.* (2022), Hei *et al.* (2016), Bendine *et al.* (2016), Ghorbanpour Arani *et al.* (2017c), Heidari and Ariaei (2022), Zhang *et al.* (2022), Luo *et al.* (2019), Wang *et al.* (2017), Dorafshan *et al.* (2013), Yang *et al.* (2013), and Chen *et al.* (2016). The analysis of wave propagation in FGM structures also has received much attention from various researchers, whose formulations have focused on applications to beams and plates (Sun and Luo, 2011; Nami and Janghorban, 2014; Aminipour and Janghorban, 2017; Aminipour *et al.*, 2018; Ellali *et al.*, 2023, 2024a, 2024b; Boucheta *et al.*, 2024; Xie *et al.*, 2023; Zhang *et al.*, 2021; Yang *et al.*, 2021).

Considering everything mentioned above, to the best of the authors' knowledge, little has been done to sufficiently investigate the impacts of the modification of material properties of the Wave propagation of the FGM plate, using the integral shear strain model. The present work offers a major contribution in the study of this effect by considering the linear exponential, quadratic, cubic, and inverse quadratic fourth functions, in addition to the commonly used power-law function P-FGM through the use of a theory presented by a displacement field that incorporates indeterminate integral terms. The use of the integral term in plate kinematics leads to a decrease in the number of unknowns and the wave propagation equations in FGM plates. It is expected that the plate consists of a mixture of metal and ceramic, whose properties change with four types of power functions across the thickness of the plate. The effects of changing material arrangement characteristics and the volume fraction of constituent plate materials on wave propagation of FGM plates with simply pressed edges are also examined.

2 Model mathematic

2.1 Material proprieties of an FGM plate

A laminated plate with thickness h is shown in Fig. 1. The present plate is prepared using a mixture of a metal level (indicated by "m") and a ceramic level (indicated by "c"), with its material composition varying smoothly along its thickness direction (i.e., in the z -axis) only. Thus, the material properties of the FGM plate, like

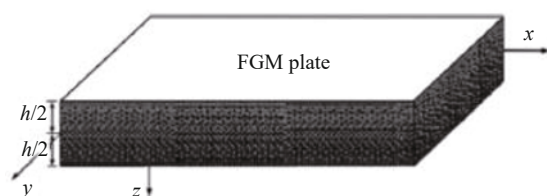


Fig. 1 A typical FGM plate

Young’s modulus E , can be expressed as:

$$P(z) = P_m + (P_c - P_m)V_c \tag{1}$$

where P_c and P_m are the material properties of the ceramic and metal, V_c represents the ceramic volume fractions, and it is assumed that the formula follows one of the following simple power-laws (Pitakthapanaphong and Busso, 2002; Bouazza *et al.*, 2018):

- (1) P-FGM: $V_c = \left(\frac{1}{2} + \frac{z}{h}\right)^k$,
- (2) Linear: $V_c = \frac{1}{2} + \frac{z}{h}$,
- (3) Quadratic: $V_c = \left(\frac{1}{2} + \frac{z}{h}\right)^2$,
- (4) Cubic: $V_c = 3\left(\frac{1}{2} + \frac{z}{h}\right)^2 - 2\left(\frac{1}{2} + \frac{z}{h}\right)^3$,
- (5) Inverse quadratic: $V_c = 1 - \left(\frac{1}{2} - \frac{z}{h}\right)^2$

2.2 Indeterminate integral variables model

The present methodology is established based on the assumptions of the inverse trigonometric shear strain theory, in which the axial displacements contain an integral component and can be given as follows (Tahir *et al.*, 2022; Hebali *et al.*, 2022; Bouafia *et al.*, 2021; Zaitoun *et al.*, 2022; Mudhaffar *et al.*, 2021; Djilali *et al.*, 2022; Ellali *et al.*, 2022b):

$$\begin{aligned} u(x, y, z, t) &= u_0(x, y, t) - z \frac{\partial w_0}{\partial x} + S_1 f(z) \int \theta(x, y, t) dx, \\ v(x, y, z, t) &= v_0(x, y, t) - z \frac{\partial w_0}{\partial y} + S_2 f(z) \int \theta(x, y, t) dy, \\ w(x, y, z, t) &= w_0(x, y, t) \end{aligned} \tag{3}$$

where t denotes time; u_0 , v_0 , w_0 and θ are the four unknowns of the displacements of the mean surface of the plate; and $f(z)$ presents the shape function, which defines the distribution of transverse shear stresses and strains throughout the thickness of the plate. The constants S_1 and S_2 depend on the geometry. In this study, we take the function $f(z)$ as follows:

$$f(z) = \sinh^{-1}\left(\frac{rz}{h}\right) - \frac{z}{h} \frac{2r}{\sqrt{r^2 + 4}}, \quad r = 3 \tag{4}$$

In the field of linear elasticity, the displacement-strain relation associated with the field for this approach

is expressed in the following form:

$$\begin{aligned} \begin{Bmatrix} \varepsilon_x \\ \varepsilon_y \\ \varepsilon_{xy} \end{Bmatrix} &= \begin{Bmatrix} \varepsilon_x^0 \\ \varepsilon_y^0 \\ \gamma_{xy}^0 \end{Bmatrix} + z \begin{Bmatrix} k_x^b \\ k_y^b \\ k_{xy}^b \end{Bmatrix} + f(z) \begin{Bmatrix} k_x^s \\ k_y^s \\ k_{xy}^s \end{Bmatrix}, \\ \begin{Bmatrix} \gamma_{xz} \\ \gamma_{yz} \end{Bmatrix} &= g(z) \begin{Bmatrix} \gamma_{xz}^0 \\ \gamma_{yz}^0 \end{Bmatrix} \end{aligned} \tag{5}$$

where

$$\begin{aligned} \begin{Bmatrix} \varepsilon_x^0 \\ \varepsilon_y^0 \\ \varepsilon_{xy}^0 \end{Bmatrix} &= \begin{Bmatrix} \frac{\partial u_0}{\partial x} \\ \frac{\partial v_0}{\partial y} \\ \frac{\partial u_0}{\partial y} + \frac{\partial v_0}{\partial x} \end{Bmatrix}, \quad \begin{Bmatrix} k_x^b \\ k_y^b \\ k_{xy}^b \end{Bmatrix} = - \begin{Bmatrix} \frac{\partial^2 w_0}{\partial x^2} \\ \frac{\partial^2 w_0}{\partial y^2} \\ 2 \frac{\partial^2 w_0}{\partial x \partial y} \end{Bmatrix}, \quad g(z) = \frac{df(z)}{dz}, \\ \begin{Bmatrix} k_x^s \\ k_y^s \\ k_{xy}^s \end{Bmatrix} &= \begin{Bmatrix} S_1 \theta \\ S_2 \theta \\ S_1 \frac{\partial}{\partial y} \int \theta dx + S_2 \frac{\partial}{\partial x} \int \theta dy \end{Bmatrix}, \quad \begin{Bmatrix} \gamma_{xz}^0 \\ \gamma_{yz}^0 \end{Bmatrix} = \begin{Bmatrix} S_1 \int \theta dx \\ S_2 \int \theta dy \end{Bmatrix} \end{aligned} \tag{6}$$

The integral terms utilized in the displacement field equations can be resolved by using Navier’s solution and can be given by:

$$\begin{aligned} \int \theta dx &= A' \frac{\partial \theta}{\partial x}, \quad \frac{\partial}{\partial y} \int \theta dx = A' \frac{\partial^2 \theta}{\partial x \partial y}, \\ \int \theta dy &= B' \frac{\partial \theta}{\partial y}, \quad \frac{\partial}{\partial x} \int \theta dy = B' \frac{\partial^2 \theta}{\partial x \partial y} \end{aligned} \tag{7}$$

Note that the integrals do not have limits. The present paper is considered using terms with integrals instead of terms with derivatives (see displacement in Sun and Luo (2011), Aminipour and Janghorban (2017)). Therefore, to better represent a new field of displacement, this paper includes indeterminate integrated terms. According to the type of solution used, the coefficients A' , B' , k_1 and k_2 are chosen, and for this contribution the Navier’s solution is used. The coefficients A' , B' , k_1 and k_2 are given as follows:

$$A' = -\frac{1}{k_1^2}, \quad B' = -\frac{1}{k_2^2}, \quad S_1 = k_1^2, \quad S_2 = k_2^2 \tag{8}$$

The constitutive equations of the plates FGM for the linear elasticity of the relation of the stresses to strains takes into account that the thermal effects are given by:

$$\begin{Bmatrix} \sigma_x \\ \sigma_y \\ \sigma_{xy} \\ \tau_{yz} \\ \tau_{xz} \end{Bmatrix} = \begin{bmatrix} Q_{11} & Q_{12} & 0 & 0 & 0 \\ Q_{21} & Q_{22} & 0 & 0 & 0 \\ 0 & 0 & Q_{66} & 0 & 0 \\ 0 & 0 & 0 & Q_{44} & 0 \\ 0 & 0 & 0 & 0 & Q_{55} \end{bmatrix} \begin{Bmatrix} \varepsilon_x \\ \varepsilon_y \\ \varepsilon_{xy} \\ \gamma_{yz} \\ \gamma_{xz} \end{Bmatrix} \quad (9)$$

where (Bouazza and Benseddiq, 2015):

$$\begin{aligned} Q_{11} = Q_{22} &= \frac{E(z)}{1-\nu(z)^2}, \quad Q_{12} = Q_{21} = \frac{\nu(z)E(z)}{1-\nu(z)^2}, \\ Q_{44} = Q_{55} = Q_{66} &= \frac{E(z)}{2[1+\nu(z)]} \end{aligned} \quad (10)$$

The resultants of stress (N_i, M_i^b, M_i^s) and (S_{xz}^s, S_{yz}^s) in the FGM plate can be expressed by integrating the corresponding stresses by means of the thickness. Such resultants of stress are given by:

$$\begin{aligned} \{N_i, M_i^b, M_i^s\} &= \int_{-\frac{h}{2}}^{\frac{h}{2}} \sigma_i \{1, z, f(z)\} dz \quad (i = x, y, xy), \\ \{S_{xz}^s, S_{yz}^s\} &= \int_{-\frac{h}{2}}^{\frac{h}{2}} g(z) \{\tau_{xz}, \tau_{yz}\} dz \end{aligned} \quad (11)$$

The resulting stresses from this proposed model can be obtained in terms of strains and stiffness elements. Replacing Eq. (9) with Eq. (11) gives us:

$$\begin{Bmatrix} N \\ M^b \\ M^s \end{Bmatrix} = \begin{bmatrix} A & B & B^s \\ B & D & D^s \\ B^s & D^s & H^s \end{bmatrix} \begin{Bmatrix} \varepsilon \\ k^b \\ k^s \end{Bmatrix} - \begin{Bmatrix} N^T \\ M^{bT} \\ M^{sT} \end{Bmatrix}, \quad S = A^s \gamma \quad (12)$$

where

$$N = \{N_x, N_y, N_{xy}\}^T, \quad M^b = \{M_x^b, M_y^b, M_{xy}^b\}^T, \quad M^s = \{M_x^s, M_y^s, M_{xy}^s\}^T,$$

$$\varepsilon = \{\varepsilon_x^0, \varepsilon_y^0, \varepsilon_{xy}^0\}^T, \quad k^b = \{k_x^b, k_y^b, k_{xy}^b\}^T, \quad k^s = \{k_x^s, k_y^s, k_{xy}^s\}^T,$$

$$S = \{S_{xz}^s, S_{yz}^s\}^T, \quad \gamma = \{\gamma_{xz}^0, \gamma_{yz}^0\}^T, \quad A^s = \begin{bmatrix} A_{44}^s & 0 \\ 0 & A_{55}^s \end{bmatrix},$$

$$\begin{aligned} A &= \begin{bmatrix} A_{11} & A_{12} & 0 \\ A_{12} & A_{22} & 0 \\ 0 & 0 & A_{66} \end{bmatrix}, \quad B = \begin{bmatrix} B_{11} & B_{12} & 0 \\ B_{12} & B_{22} & 0 \\ 0 & 0 & B_{66} \end{bmatrix}, \quad B^s = \begin{bmatrix} B_{11}^s & B_{12}^s & 0 \\ B_{12}^s & B_{22}^s & 0 \\ 0 & 0 & B_{66}^s \end{bmatrix}, \\ D &= \begin{bmatrix} D_{11} & D_{12} & 0 \\ D_{12} & D_{22} & 0 \\ 0 & 0 & D_{66} \end{bmatrix}, \quad D^s = \begin{bmatrix} D_{11}^s & D_{12}^s & 0 \\ D_{12}^s & D_{22}^s & 0 \\ 0 & 0 & D_{66}^s \end{bmatrix}, \quad H^s = \begin{bmatrix} H_{11}^s & H_{12}^s & 0 \\ H_{12}^s & H_{22}^s & 0 \\ 0 & 0 & H_{66}^s \end{bmatrix} \end{aligned} \quad (13)$$

The stiffness terms of this approach are defined as follows:

$$\begin{aligned} \{A_{ij}, B_{ij}, D_{ij}, B_{ij}^s, D_{ij}^s, H_{ij}^s\} &= \\ \int_{-\frac{h}{2}}^{\frac{h}{2}} Q_{ij} \{1, z, z^2, f(z), zf(z), [f(z)]^2\} dz \quad (i, j = 1, 2, 6), \\ A_{44}^s &= \int_{-\frac{h}{2}}^{\frac{h}{2}} Q_{44} [g(z)]^2 dz, \quad A_{55}^s = \int_{-\frac{h}{2}}^{\frac{h}{2}} Q_{55} [g(z)]^2 dz \end{aligned} \quad (14)$$

With this contribution, we use Hamilton's principle to obtain the equations of motion. This principle can be given in analytical form as follows (Ghorbanpour Arani et al., 2017a):

$$\int_0^t (\delta U - \delta K) dt = 0 \quad (15)$$

where δU represents the change in strain energy, while δK represents the change in kinetic energy.

$$\begin{aligned} \delta U &= \int_V (\sigma_x \delta \varepsilon_x + \sigma_y \delta \varepsilon_y + \sigma_{xy} \delta \varepsilon_{xy} + \tau_{xz} \delta \gamma_{xz} + \tau_{yz} \delta \gamma_{yz}) dV \\ &= \int_A (N_x \delta \varepsilon_x^0 + N_y \delta \varepsilon_y^0 + N_{xy} \delta \varepsilon_{xy}^0 + M_x^b \delta k_x^b + M_y^b \delta k_y^b + \\ &M_{xy}^b \delta k_{xy}^b + M_x^s \delta k_x^s + M_y^s \delta k_y^s + M_{xy}^s \delta k_{xy}^s + S_{xz}^s \delta \gamma_{xz}^s + S_{yz}^s \delta \gamma_{yz}^s) dA \end{aligned} \quad (16)$$

$$\begin{aligned} \delta K &= \int_V (\dot{u} \delta \dot{u} + \dot{v} \delta \dot{v} + \dot{w} \delta \dot{w}) \rho(z) dV = \\ &\int_A \{I_0 (\dot{u}_0 \delta \dot{u}_0 + \dot{v}_0 \delta \dot{v}_0 + \dot{w}_0 \delta \dot{w}_0) - \\ &I_1 \left(\dot{u}_0 \frac{\partial \delta \dot{w}_0}{\partial x} + \frac{\partial \dot{w}_0}{\partial x} \delta \dot{u}_0 + \dot{v}_0 \frac{\partial \delta \dot{w}_0}{\partial y} + \frac{\partial \dot{w}_0}{\partial y} \delta \dot{v}_0 \right) + \\ &J_1 \left[S_1 A' \left(\dot{u}_0 \frac{\partial \delta \dot{\theta}}{\partial x} + \frac{\partial \dot{\theta}}{\partial x} \delta \dot{u}_0 \right) + S_2 B' \left(\dot{v}_0 \frac{\partial \delta \dot{\theta}}{\partial y} + \frac{\partial \dot{\theta}}{\partial y} \delta \dot{v}_0 \right) \right] + \\ &I_2 \left(\frac{\partial \delta \dot{w}_0}{\partial x} \frac{\partial \dot{w}_0}{\partial x} + \frac{\partial \delta \dot{w}_0}{\partial y} \frac{\partial \dot{w}_0}{\partial y} \right) - J_2 \left[S_1 A' \left(\frac{\partial \dot{w}_0}{\partial x} \frac{\partial \delta \dot{\theta}}{\partial x} + \frac{\partial \dot{\theta}}{\partial x} \frac{\partial \delta \dot{w}_0}{\partial x} \right) + \right. \\ &S_2 B' \left. \left(\frac{\partial \dot{w}_0}{\partial y} \frac{\partial \delta \dot{\theta}}{\partial y} + \frac{\partial \dot{\theta}}{\partial y} \frac{\partial \delta \dot{w}_0}{\partial y} \right) \right] + J_3 \left[(S_1 A')^2 \left(\frac{\partial \delta \dot{\theta}}{\partial x} \frac{\partial \dot{\theta}}{\partial x} \right) + (S_2 B')^2 \left(\frac{\partial \delta \dot{\theta}}{\partial y} \frac{\partial \dot{\theta}}{\partial y} \right) \right] \} dA \end{aligned} \quad (17)$$

where the dot-superscript convention implies the differentiation concerning the time t , $\rho(z)$ denotes mass density, and (I, J) are the mass inertias as defined by:

$$\begin{aligned} \{I_0, I_1, I_2\} &= \int_{-\frac{h}{2}}^{\frac{h}{2}} \{1, z, z^2\} \rho(z) dz, \\ \{J_1, J_2, J_3\} &= \int_{-\frac{h}{2}}^{\frac{h}{2}} \{f(z), zf(z), f(z)^2\} \rho(z) dz \end{aligned} \quad (18)$$

By replacing the expressions of the stress and the deformations of Eqs. (16) and (17) with Eq. (15), and integrating by parts while separately isolating the coefficients u_0 , v_0 , w_0 , and θ , we obtain the equilibrium equations as follows:

$$\begin{aligned}
 \delta u_0 : & \frac{\partial N_x}{\partial x} + \frac{\partial N_{xy}}{\partial y} = I_0 \ddot{u}_0 - I_1 \frac{\partial \ddot{w}_0}{\partial x} + S_1 A' J_1 \frac{\partial \ddot{\theta}}{\partial x}, \\
 \delta v_0 : & \frac{\partial N_{xy}}{\partial x} + \frac{\partial N_y}{\partial y} = I_0 \ddot{v}_0 - I_1 \frac{\partial \ddot{w}_0}{\partial y} + S_2 B' J_1 \frac{\partial \ddot{\theta}}{\partial y}, \\
 \delta w_0 : & \frac{\partial^2 M_x^b}{\partial x^2} + 2 \frac{\partial^2 M_{xy}^b}{\partial x \partial y} + \frac{\partial^2 M_y^b}{\partial y^2} = \\
 & I_0 \ddot{w}_0 + I_1 \left(\frac{\partial \ddot{u}_0}{\partial x} + \frac{\partial \ddot{v}_0}{\partial y} \right) - I_2 \left(\frac{\partial^2 \ddot{w}_0}{\partial x^2} + \frac{\partial^2 \ddot{w}_0}{\partial y^2} \right) + \\
 & J_2 \left(S_1 A' \frac{\partial^2 \ddot{\theta}}{\partial x^2} + S_2 B' \frac{\partial^2 \ddot{\theta}}{\partial y^2} \right), \\
 \delta \theta : & -S_1 M_x^s - S_2 M_y^s - (S_1 A' + S_2 B') \frac{\partial^2 M_{xy}^s}{\partial x \partial y} + S_1 A' \frac{\partial S_{xz}^s}{\partial x} + S_2 B' \frac{\partial S_{yz}^s}{\partial y} = \\
 & -J_1 \left(S_1 A' \frac{\partial \ddot{u}_0}{\partial x} + S_2 B' \frac{\partial \ddot{v}_0}{\partial y} \right) + J_2 \left(S_1 A' \frac{\partial^2 \ddot{w}_0}{\partial x^2} + S_2 B' \frac{\partial^2 \ddot{w}_0}{\partial y^2} \right) \\
 & -J_3 \left[(S_1 A')^2 \frac{\partial^2 \ddot{\theta}}{\partial x^2} + (S_2 B')^2 \frac{\partial^2 \ddot{\theta}}{\partial y^2} \right] \tag{19}
 \end{aligned}$$

We assume solutions for u_0, v_0, w_0 and θ as representing waves propagating in the x - y plane in the form (Sun and Luo, 2011):

$$\begin{Bmatrix} u_0(x, y, t) \\ v_0(x, y, t) \\ w_0(x, y, t) \\ \theta(x, y, t) \end{Bmatrix} = \begin{Bmatrix} U \cdot \exp[i(k_1 x + k_2 y - \omega t)] \\ V \cdot \exp[i(k_1 x + k_2 y - \omega t)] \\ W \cdot \exp[i(k_1 x + k_2 y - \omega t)] \\ X \cdot \exp[i(k_1 x + k_2 y - \omega t)] \end{Bmatrix} \tag{20}$$

where U, V, W and X denote the coefficients of the amplitude of the wave, k_1 and k_2 are the wavenumbers of wave propagation along the x -axis and y -axis directions, respectively, and ω denotes the frequency

$$(\mathbf{K} - \omega^2 \mathbf{M}) \mathbf{\Delta} = \mathbf{0} \tag{21}$$

where

$$\mathbf{\Delta} = \{U, V, W, X\}^T \tag{22}$$

By substituting Eq. (20) with Eq. (19), we obtain:

$$\left(\begin{bmatrix} S_{11} & S_{12} & S_{13} \\ S_{21} & S_{22} & S_{23} \\ S_{31} & S_{32} & S_{33} \\ S_{41} & S_{42} & S_{43} \end{bmatrix} - \omega^2 \begin{bmatrix} m_{11} & m_{12} & m_{13} \\ m_{21} & m_{22} & m_{23} \\ m_{31} & m_{32} & m_{33} \\ m_{41} & m_{42} & m_{43} \end{bmatrix} \right) \begin{Bmatrix} U \\ V \\ W \\ X \end{Bmatrix} = \begin{Bmatrix} 0 \\ 0 \\ 0 \\ 0 \end{Bmatrix} \tag{23}$$

The dispersion relations of the wave propagation in the FGM plate are presented by

$$|\mathbf{K} - \omega^2 \mathbf{M}| = 0 \tag{24}$$

Assuming $k_1 = k_2 = k$, the roots of Eq. (24) can be given as:

$$\omega_i = W_i(k), \quad i = 1, 2, 3, 4 \tag{25}$$

They communicate to the wave modes M_1, M_2, M_3 and M_4 , respectively. M_1 and M_4 wave modes correspond to the bending wave, and the M_2 and M_3 wave modes correspond to the extension wave. The wave propagation phase velocity in the FGM plate can be stated by:

$$C_i = \frac{W_i(k)}{k}, \quad i = 1, 2, 3, 4 \tag{26}$$

3 Numerical results and discussion

3.1 Comparison of results

In this part, several numerical examples are studied and discussed to verify the accuracy of the new theory via indeterminate integral variables with an inverse sine hyperbolic shape function in the prediction of wave propagations of functionally graduated plates. The results obtained by the use of this theory are compared with those of theories, such as classical plate theory (CPT), first-order shear deformation theory (FSDT), higher-order shear deformation theory (HSDT), higher-order shear strain theory (HOSST), and third-order shear deformation theory (TSDT).

First, we analyze a simply supported isotropic square plate. This analysis is carried out for a plate with a thickness 2 mm and mechanical characteristics ($\rho=7480 \text{ kg/m}^3, E=210 \text{ GPa}, \nu=0.3$), and for different wavenumber values of $k=k_1=k_2$. The results are reported in Table 1. The outcomes obtained by the use of the current theory are compared to the results from the closed-form solution distributed by Nami and Janghorban (2014), which were based on the classical theory of plates and data available in published literature as obtained by Aminipour *et al.* (2018), which in turn were based on higher-order shear strain theory. The comparison shows good agreement between the three cases.

Still, to validate the results of the wave propagation one must carry out a comparison of frequencies related to modes M_1 and M_4 of an isotropic square plate simply supported with a thickness 0.02 m and mechanical characteristics ($\rho=7480 \text{ kg/m}^3, E=210 \text{ GPa}, \nu=0.3$) and for different wavenumber values with $k=k_1=k_2$. The values obtained by using the present variable indeterminate integral theory with the hyperbolic arcsine shape function are also compared to the results of Aminipour

Table 1 Comparison of the results of the frequencies of the mode M_1 . The case of a simply supported square isotropic plate with $h = 2$ mm, wavenumber $k=k_1=k_2$, $\rho=7480$ kg/m³, $E=210$ GPa, $\nu=0.3$

Theory	k									
	5	10	15	20	25	30	40	50	75	100
HOSST ^a	160.336	641.28	1442.61	2564.00	4004.96	5764.87	10238.39	15976.97	35789.62	63239.08
CPT ^b	160.342	641.37	1443.08	2565.47	4008.55	5772.32	10261.89	16034.21	36076.97	64136.83
Present	160.336	641.28	1442.61	2563.99	4004.93	5764.81	10238.21	15976.53	35787.40	63232.19

Note: ^aAminipour *et al.* (2018), ^bNami and Janghorban (2014).

Table 2 Comparison of the results of the circular frequencies of the modes. The case of a simply supported square isotropic plate $h = 0.02$ m, wavenumber $k=k_1=k_2$, $\rho=7480$ kg/m³, $E=210$ GPa, $\nu=0.3$

k	Mode (01)			Mode (i)		
	Present	HOSST ^a	TSDT ^b	Present	HOSST ^a	TSDT ^b
1	64.13	64.13	64.23	516579.15	521261.66	516246.77
3	576.47	576.49	577.41	517192.35	521869.59	516866.97
5	1597.54	1597.70	1600.16	518415.07	523081.86	518103.70
7	3120.27	3120.86	3125.43	520240.09	524891.41	519949.78
9	5134.31	5135.89	5142.89	522656.86	527287.94	522394.66
11	7626.37	7629.83	7639.29	525651.81	530258.18	525424.84
13	10580.61	10587.24	10598.83	529208.75	533786.30	529024.19
15	13979.06	13990.57	14003.60	533309.30	537854.31	533174.41
17	17802.08	17820.66	17834.04	537933.34	542442.49	537855.47
20	24286.86	24321.12	24332.19	545803.93	550253.95	545825.60
25	36913.44	36991.33	36987.99	561226.23	565566.82	561452.39
30	51517.44	51666.69	51631.75	579223.26	583445.63	579704.49
35	67775.30	68029.61	67942.46	599457.77	603557.60	600247.88
40	85397.08	85795.13	85633.10	621624.15	625600.48	622780.64
45	104132.79	104717.40	104456.78	645455.09	649309.21	647039.46
50	123772.52	124590.00	124206.70	670721.91	674456.55	672799.75
55	144143.08	145242.79	144712.72	697231.45	700850.25	699872.52
60	165103.31	166537.39	165836.55	724821.65	728328.72	728099.80
65	186539.04	188362.24	187466.67	753356.77	756756.43	757349.76
70	208358.46	210628.05	209513.65	782722.92	786019.56	787512.26
75	230488.02	233263.71	231906.00	812824.24	816022.20	818494.96
80	252868.99	256212.90	254586.76	843579.61	846683.11	850219.95

Note: ^aAminipour *et al.* (2018), ^bAminipour and Janghorban (2017), (i) Mode (04) for Present, (i) Mode (05) for HOSST^a and TSDT^b

and Janghorban (2017) and Aminipour *et al.* (2018). It is stated that the frequencies of the M_4 mode gained from this study are contrasted with the M_5 modes obtained by Aminipour *et al.* (2018) and Aminipour and Janghorban (2017), as the new four-variable theory introduces indeterminate integral variables, while the models of Aminipour and Janghorban (2017) and Aminipour *et al.* (2018) contain five variables. From Table 2 we find that our results are in good agreement with those available results for wave propagation in isotropic plates.

In the third comparison, wave propagation in a functionally graded (FG) plate that consists of a mixture

of silicon nitride (Si_3N_4) ceramic and stainless steel (SUS304) metal constitute the materials in the upper and lower surfaces of the FGM plate, respectively. The properties of the ceramic and the metal are provided in Table 4. The results are illustrated in Table 3. This comparison also is carried out using the results of Sun and Luo (2011) and the results of Aminipour *et al.* (2018) under thermal environmental conditions $T_b = T_t = 300$ K. We notice that the results obtained by Sun and Luo (2011) and Aminipour *et al.* (2018) and the present theory are in great agreement for distinct volume fraction indices.

Table 3 Comparison of the results of the mode frequencies. The case of a simply supported FGM plate, material Si₃N₄/SUS304 in thermal environmental conditions $T_b=T_t=300$ K (Sun and Luo, 2011)

k	N											
	0			0.5			1			2		
	Aminipour <i>et al.</i> (2018)	Sun and Lou (2011)	Present	Aminipour <i>et al.</i> (2018)	Sun and Lou (2011)	Present	Aminipour <i>et al.</i> (2018)	Sun and Lou (2011)	Present	Aminipour <i>et al.</i> (2018)	Sun and Lou (2011)	Present
20	52758.57	52.6899	52.7389	36572.35	36.5236	36.5580	32134.22	32.0916	32.1219	28,886.10	28.8495	28.8747
30	112408.02	112.1074	112.3230	77814.20	77.6051	77.7545	68311.13	68.1256	68.2584	61,302.08	61.1407	61.2531
40	187238.35	186.4332	187.0144	129427.56	128.8765	129.2735	113518.57	113.0247	113.3806	101,690.08	101.2544	101.5612
50	272701.67	271.0430	272.2490	188248.29	187.1288	187.9414	164973.83	163.9613	164.6967	147,536.97	146.6312	147.2766
60	365473.56	362.5580	364.6936	251989.82	250.0447	251.4674	220681.79	218.9086	220.2068	197,063.64	195.4564	196.6148
70	463288.52	458.6690	462.0776	319111.09	316.0583	318.3079	279308.89	276.5064	278.5745	249,096.62	246.5266	248.3987
80	564654.89	557.8450	562.9057	388607.51	384.1406	387.4562	339993.49	335.8684	338.9356	302,889.03	299.0677	301.8785
90	668609.41	659.0849	666.2111	459835.71	453.6233	458.2669	402189.39	396.4238	400.7416	35976.27	352.5894	356.5868
100	774540.38	761.7401	771.3784	532389.66	524.0754	530.3316	465556.32	457.8079	463.6497	414,076.15	406.7849	412.2388

Table 4 Properties of Si₃N₄ and SUS304 in thermal environmental conditions $T_b=T_t=300$ K (Sun and Luo, 2011)

Material	Properties		
	E (GPa)	ν	ρ (kg/m ³)
Ceramic (Si ₃ N ₄)	348.43	0.24	2370
Metal (SUS304)	201.04	0.3262	8166

3.2 Parametric study

The outcomes of the numerical calculations in this part are shown in Figs. 2–5. The FGM material used Si₃N₄/SUS304 for thermal conditions $T_b = T_t = 300$ K.

The variations of the four modes of dispersion curves for homogeneous and functionally graduated plates concerning the numbers of propagation waves for all composition profiles are shown in Fig. 2. SUS304 and Si₃N₄ correspond to all-metal plates and all-ceramic

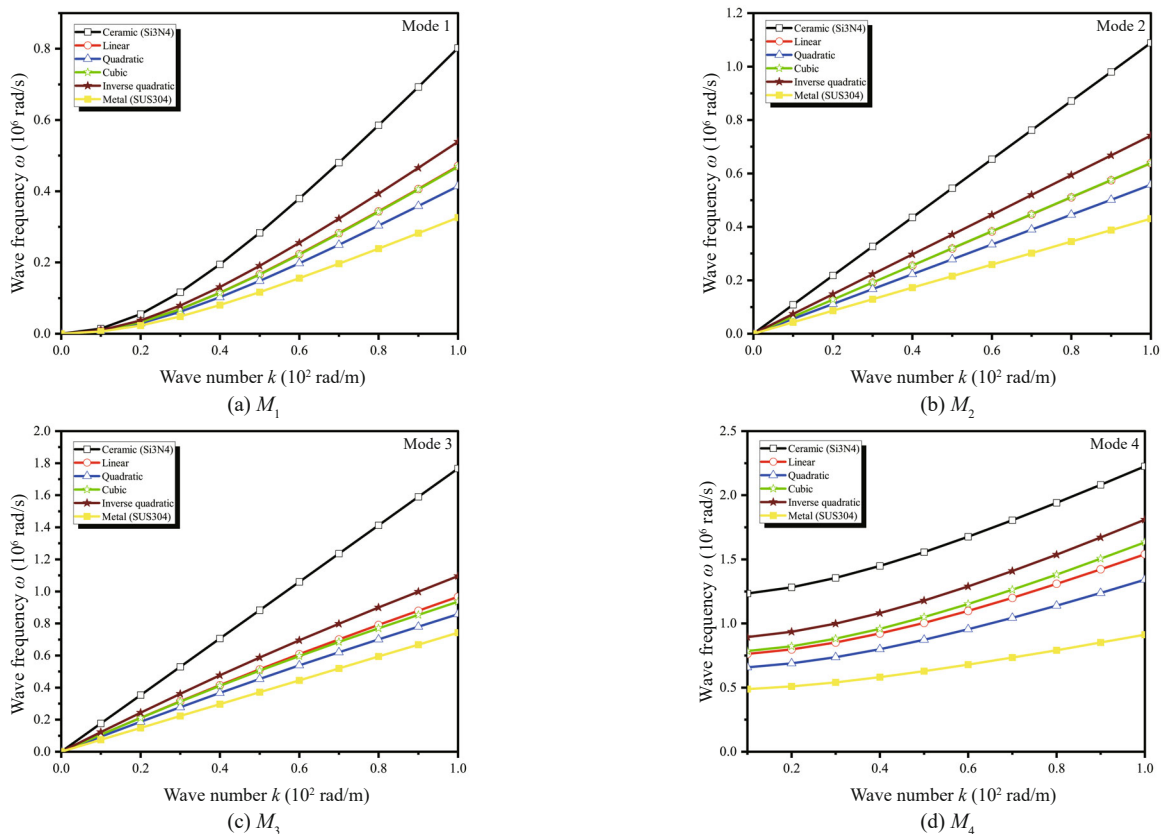


Fig. 2 The dispersion curves of various functionally graded plates with $T_b=T_t=300$ K

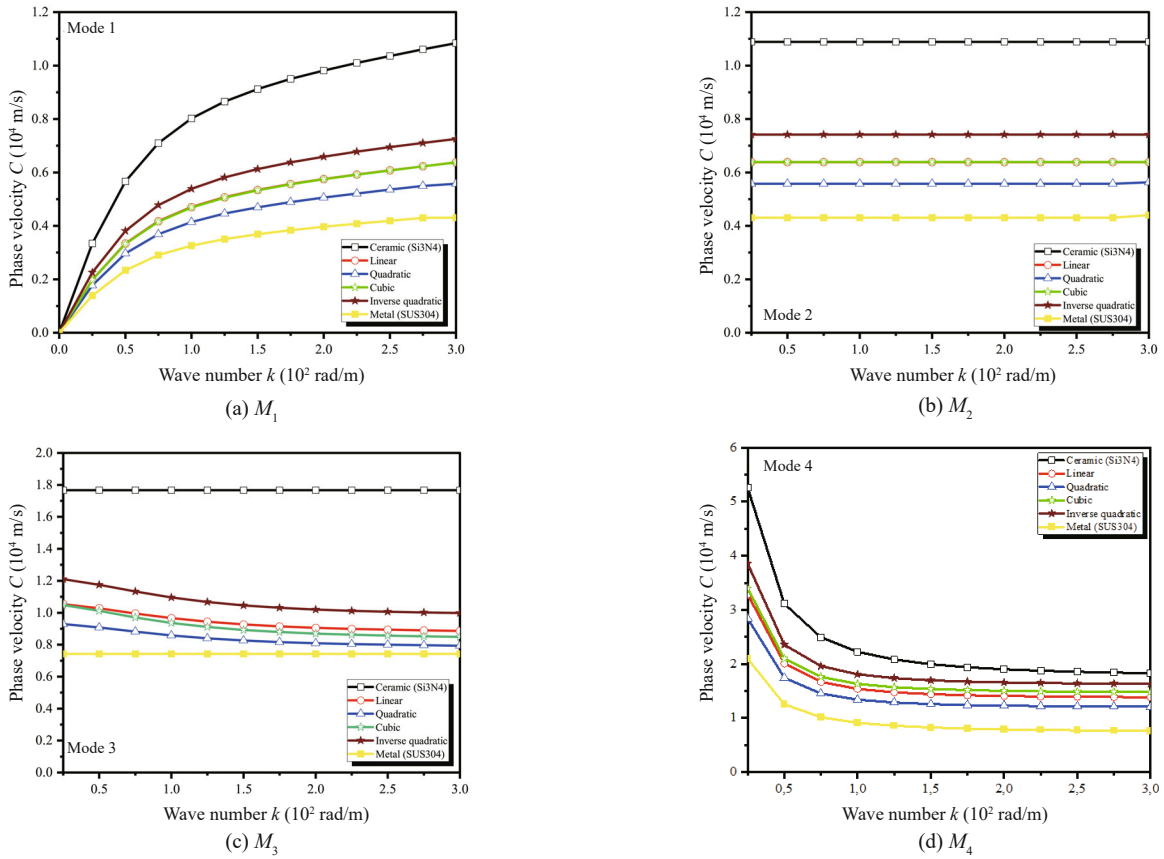


Fig. 3 The phase velocity curves of various functionally graded plates $T_b=T_t=300$ K

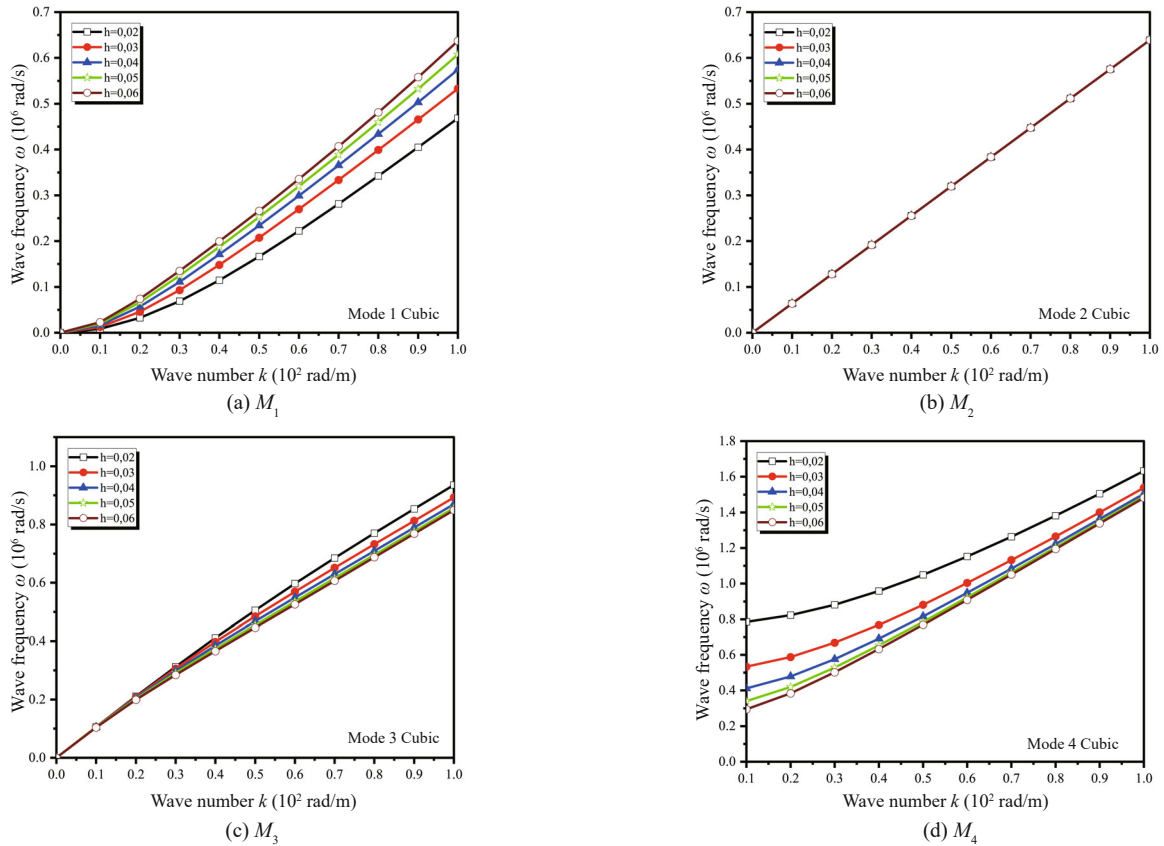


Fig. 4 The dispersion curves of various functionally graded plates with $T_b=T_t=300$ K

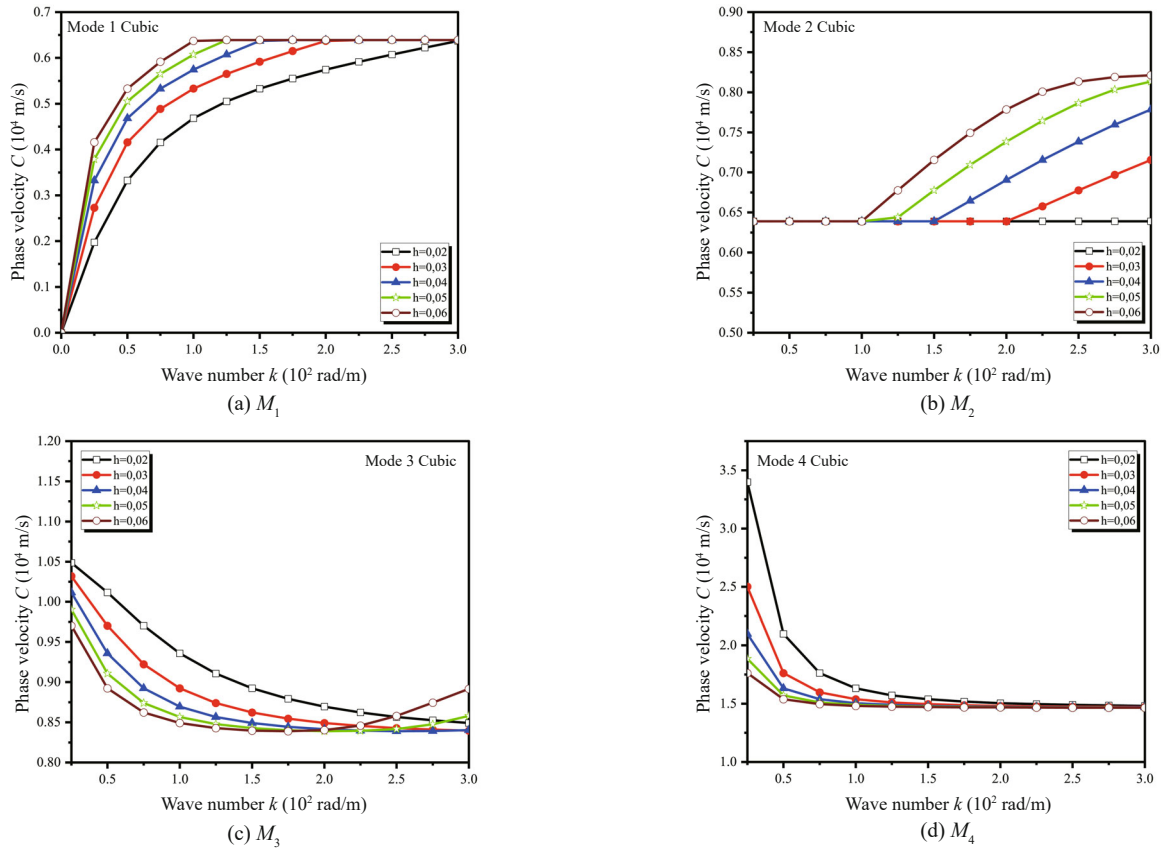


Fig. 5 The phase velocity curves of various functionally graded plates $T_b=T_t=300\text{ K}$

plates, respectively. But in the other cases, the linear, quadratic, and inverse quadratic profile composition is for the graduated plates with two constituent materials, $\text{Si}_3\text{N}_4/\text{SUS304}$. Figure 2 shows that the dispersion curves of the FGM plates are lower than those of the all-ceramic plates, but higher than those of the all-metal plates. The dispersion curves were taken from the composition profile at a quadratic lower than the linear, cubic, and inverse quadratic cases. The dispersion curves were obtained from the composition profile with a quadratic inverse greater than the linear and cubic cases. In all material cases, the dispersion curves increase when the number of wave propagation waves also increase. For modes 1, 2, and 3, the lines corresponding to the compositional case of the cubic profile coincide with the lines for the linear compositional profile; however, for mode 4, the cubic compositional case of the profile is greater than that of the linear compositional profile.

Figure 3 shows the variation of phase velocity with respect to the wavenumber (k) for various volume fractions and different modes M_1 , M_2 , M_3 and M_4 . It is observed that with an increase in the number of modes of the plate from mode 1 to mode 4, the phase velocity increases regularly. It is also found that the phase velocity curves of the FG plates are higher than those of fully metal plates but lower than those of fully ceramic plates. However, we see that the values of the quadratic case

are lower than the phase velocity values of the cubic, linear and inverse quadratic cases, whereas the values of the cubic and linear cases are greater than the phase velocity values of the quadratic case. In addition, the line corresponding to the case of the cubic composition profile coincides with the lines of the linear composition profiles for modes 1, 2 and 3. However, for mode 4, we see that the values of the cubic case are greater than those of the phase velocity of the linear case.

Figure 4 shows the changes in wave frequencies for the wavenumbers of FGM plates for different thicknesses. We can see from these graphs that the wave frequencies increase with an increase in thickness (h) for the M_1 mode. It also can be noted that for the M_2 wave mode, regardless of the thickness value, the wave frequencies are almost identical. The figure also shows that the effect of thickness on wave frequencies in the cubic type can be reversed as the mode increases; then the M_3 and M_4 modes decrease with the increasing thickness (h) of the FGM plates.

The variations of the curves of phase velocity vs wavenumber for the cubic composition profile are shown in Fig. 5. It can be seen that phase velocity increased with increasing thickness for M_1 and M_2 . Also, this effect can be reversed as the mode increases for M_3 and M_4 .

4 Conclusions

This contribution presents an analytical model based on a high order theory and new displacement field with four unknowns, while introducing indeterminate integral variables and a hyperbolic inverse sine function to study the propagation of the waves of FGM plates. It is presumed that the plate is a mixture of metal (SUS304) and ceramic (Si_3N_4) and that its properties change according to the thickness of the plate. Applying the method and the Navier procedure, the dispersion and phase velocity of the FGM plates are achieved. The formulas for the case of homogeneous isotropic plaques are found as a special case. The influences of volume fraction and the composition of constituent materials and the variation in plate thickness on dispersion and phase velocity are also studied. The results are compared to their counterparts in the literature. The following remarks pertain to this research:

(1) The study of wave propagation interests different fields related to civil engineering: earthquake engineering, vibration isolation, non-destructive testing, etc. Wave propagation problems are characterized by different phenomena, dispersion, diffraction, damping, wave type conversions, etc.

(2) The use of indeterminate integral terms allows for the reduction of the number of variables and the equations of propagation, thereby making the model simple and efficient to use.

(3) Wave propagation frequency and the phase velocity in the graduated plate are functionally influenced by the type of volume fraction distributions.

(4) Wave propagation frequency and the phase velocity in FGM plates are higher than those of all metal plates but lower than those of all ceramic ones.

(5) The impact of the heterogeneity of the functionally graduated materials on wave propagation in the functionally graduated plate is great. When the values of wave propagation frequency and phase velocity of FGM plates are compared with those of a homogeneous metal plate; the least impact is encountered in the quadratic case; the maximum impact is found in the inverse quadratic case.

(6) The thickness variation has an obvious influence on wave propagation frequency values and the phase velocity of functionally graduated plates, an influence that depends on the wave modes.

Due to the interesting features of the present approach, these findings will serve as a useful benchmark for evaluating the reliability of other future FGM plate models. Additionally, future work is needed to solve the problems of wave propagation for a functionally graded plate through the use of the integral variables model to take into account the effects of damping and temperature-dependent material properties.

References

Al-Furjan MSH, Fan S, Shan L, Farrokhan A, Shen X

and Kolahchi R (2023), "Wave Propagation Analysis of Micro Air Vehicle Wings with Honeycomb Core Covered by Porous FGM and Nanocomposite Magnetostrictive Layers," *Waves in Random and Complex Media*, Online. <https://doi.org/10.1080/17455030.2022.2164378>

Al-Furjan MSH, Xu MX, Farrokhan A, Jafari GS, Shen X and Kolahchi R (2022a), "On Wave Propagation in Piezoelectric-Auxetic Honeycomb-2D-FGM Micro-Sandwich Beams Based on Modified Couple Stress and Refined Zigzag Theories," *Waves in Random and Complex Media*, Online. <https://doi.org/10.1080/17455030.2022.2030499>

Al-Furjan MSH, Yang Y, Farrokhan A, Shen X, Kolahchi R and Rajak DK (2022b), "Dynamic Instability of Nanocomposite Piezoelectric-Leptadenia Pyrotechnica Rheological Elastomer-Porous Functionally Graded Materials Micro Viscoelastic Beams at Various Strain Gradient Higher-Order Theories," *Polymer Composites*, **43**(1): 282–298. <https://doi.org/10.1002/pc.26373>

Al-Furjan MSH, Yin C, Shen X, Kolahchi R, Zarei MS and Hajmohammad MH (2022c), "Energy Absorption and Vibration of Smart Auxetic FG Porous Curved Conical Panels Resting on the Frictional Viscoelastic Torsional Substrate," *Mechanical Systems and Signal Processing*, **178**: 109269. <https://doi.org/10.1016/j.ymssp.2022.109269>

Aminipour H and Janghorban M (2017), "Wave Propagation in Anisotropic Plates Using Trigonometric Shear Deformation Theory," *Mechanics Advanced Materials and Structures*, **24**(13): 1135–1144.

Aminipour H, Janghorban M and Li L (2018), "A New Model for Wave Propagation in Functionally Graded Anisotropic Doubly-Curved Shells," *Composite Structures*, **190**: 91–111.

Bakoura A, Bourada F, Bousahla AA, Tounsi A, Benrahou KH, Tounsi A, Al-Zahrani MM and Mahmoud SR (2021), "Buckling Analysis of Functionally Graded Plates Using HSDT in Conjunction with the Stress Function Method," *Computers and Concrete*, **27**(1): 73–83. <https://doi.org/10.12989/cac.2021.27.1.073>

Becheri T, Amara K, Bouazza M and Benseddiq N (2016), "Buckling of Symmetrically Laminated Plates Using n th-Order Shear Deformation Theory with Curvature Effects," *Steel and Composite Structures*, **21**(6): 1347–1368. <https://doi.org/10.12989/SCS.2016.21.6.1347>

Belmahi S, Zidour M, Meradjah M, Bensattalah T and Dihaj A (2018), "Analysis of Boundary Conditions Effects on Vibration of Nanobeam in a Polymeric Matrix," *Structural Engineering and Mechanics*, **67**(5): 517–525. <https://doi.org/10.12989/sem.2018.67.5.517>

Bendine K, Boukhoulda FB, Nouari M and Sarla Z (2016), "Active Vibration Control of Functionally Graded Beams with Piezoelectric Layers Based on Higher Order Shear Deformation Theory," *Earthquake Engineering and Engineering Vibration*, **15**(4): 611–

620. <https://doi.org/10.1007/s11803-016-0352-y>

Benedjadi M, Aldosari SM, Chikh A, Kaci A, Bousahla AA, Bourada F, Tounsi A, Benrahou KH and Tounsi A (2023), “Visco-Elastic Foundation Effect on Buckling Response of Exponentially Graded Sandwich Plates Under Various Boundary Conditions,” *Geomechanics and Engineering*, **32**(2): 159–177. <https://doi.org/10.12989/gae.2023.32.2.159>

Bot IK, Bousahla AA, Zemri A, Sekkal M, Kaci A, Bourada F, Tounsi A, Ghazwani MH and Mahmoud SR (2022), “Effects of Pasternak Foundation on the Bending Behavior of FG Porous Plates in Hygrothermal Environment,” *Steel and Composite Structures*, **43**(6): 821–837. <https://doi.org/10.12989/scs.2022.43.6.821>

Bouafia K, Selim MM, Bourada F, Bousahla AA, Bourada M, Tounsi A, Bedia EAA and Tounsi A (2021), “Bending and Free Vibration Characteristics of Various Compositions of FG Plates on Elastic Foundation via Quasi 3D HSDT Model,” *Steel and Composite Structures*, **41**(4): 487–503. <https://doi.org/10.12989/SCS.2021.41.4.487>

Bouazza M, Antar K, Amara K, Benyoucef S and Bedia EAA (2019a), “Influence of Temperature on the Beams Behavior Strengthened by Bonded Composite Plates,” *Geomechanics and Engineering*, **18**(5): 555–566. <https://doi.org/10.12989/GAE.2019.18.5.555>

Bouazza M, Becheri T, Boucheta A and Benseddiq N (2016), “Thermal Buckling Analysis of Nanoplates Based on Nonlocal Elasticity Theory with Four-Unknown Shear Deformation Theory Resting on Winkler-Pasternak Elastic Foundation,” *International Journal for Computational Methods in Engineering Sciences and Mechanics*, **17**(5–6): 362–373. <https://doi.org/10.1080/15502287.2016.1231239>

Bouazza M, Becheri T, Boucheta A and Benseddiq N (2019b), “Bending Behavior of Laminated Composite Plates Using the Refined Four-Variable Theory and the Finite Element Method,” *Earthquakes and Structures*, **17**(3): 257–270. <https://doi.org/10.12989/EAS.2019.17.3.257>

Bouazza M and Benseddiq N (2015), “Analytical Modeling for the Thermoelastic Buckling Behavior of Functionally Graded Rectangular Plates Using Hyperbolic Shear Deformation Theory Under Thermal Loadings,” *Multidiscipline Modeling in Materials and Structures*, **11**(4): 558–578. <https://doi.org/10.1108/MMMS-02-2015-0008>

Bouazza M, Kenouza Y, Benseddiq N and Zenkour AM (2017), “A Two-Variable Simplified n th-Higher-Order Theory for Free Vibration Behavior of Laminated Plates,” *Composite Structures*, **182**: 533–541. <https://doi.org/10.1016/j.compstruct.2017.09.041>

Bouazza M and Zenkour AM (2018), “Free Vibration Characteristics of Multilayered Composite Plates in a Hygrothermal Environment via the Refined Hyperbolic Theory,” *The European Physical Journal Plus*, **133**: 217. <https://doi.org/10.1140/epjp/i2018-12050-x>

Bouazza M and Zenkour AM (2020), “Hygro-Thermo-Mechanical Buckling of Laminated Beam Using Hyperbolic Refined Shear Deformation Theory,” *Composite Structures*, **252**: 112689. <https://doi.org/10.1016/j.compstruct.2020.112689>

Bouazza M and Zenkour AM (2021), “Vibration of Inhomogeneous Fibrous Laminated Plates Using an Efficient and Simple Polynomial Refined Theory,” *Journal of Computational Applied Mechanics*, **52**(2): 233–245. <https://doi.org/10.22059/jcamech.2021.320751.605>

Bouazza M and Zenkour AM (2024), “Hygrothermal Environmental Effect on Free Vibration of Laminated Plates Using n th-Order Shear Deformation Theory,” *Waves in Random and Complex Media*, **34**(1): 307–323. <https://doi.org/10.1080/17455030.2021.1909173>

Bouazza M, Zenkour AM and Benseddiq N (2018), “Effect of Material Composition on Bending Analysis of FG Plates via a Two-Variable Refined Hyperbolic Theory,” *Archives of Mechanics*, **70**(2): 107–129.

Boucheta A, Bouazza M, Becheri T, Eltahir MA, Tounsi A and Benseddiq N (2024), “Bending of Sandwich FGM Plates with a Homogeneous Core Either Hard or Soft via a Refined Hyperbolic Shear Deformation Plate Theory,” *Iranian Journal of Science and Technology, Transactions of Civil Engineering*, Online. <https://doi.org/10.1007/s40996-024-01386-w>

Chen JT, Lee JW and Tu YC (2016), “Focusing Phenomenon and Near-Trapped Modes of SH Waves,” *Earthquake Engineering and Engineering Vibration*, **15**(3): 477–486. <https://doi.org/10.1007/s11803-016-0337-x>

Chen PJ, Guo W, Zhao YC, Li EX, Yang YG and Liu H (2019), “Numerical Analysis of the Strength and Interfacial Properties of Adhesive Joints with Graded Adherends,” *International Journal of Adhesion and Adhesives*, **90**: 88–96. <https://doi.org/10.1016/j.ijadhadh.2019.02.003>

Chu CC, Al-Furjan MSH, Kolahchi R and Farrokhanian A (2023), “A Nonlinear Chebyshev-Based Collocation Technique to Frequency Analysis of Thermally Pre/Post-Buckled Third-Order Circular Sandwich Plates,” *Communications in Nonlinear Science and Numerical Simulation*, **118**: 107056. <https://doi.org/10.1016/j.cnsns.2022.107056>

Derbale A, Bouazza M and Benseddiq N (2021), “Analysis of the Mechanical and Thermal Buckling of Laminated Beams by New Refined Shear Deformation Theory,” *Iranian Journal of Science and Technology, Transactions of Civil Engineering*, **45**: 89–98. <https://doi.org/10.1007/s40996-020-00417-6>

Dihaj A, Zidour M, Meradjah M, Rakrak K, Heireche H and Chemi A (2018), “Free Vibration Analysis of Chiral Double-Walled Carbon Nanotube Embedded in an Elastic Medium Using Non-Local Elasticity Theory and Euler Bernoulli Beam Model,” *Structural Engineering and Mechanics*, **65**(3): 335–342. <http://dx.doi.org/10.12989/sem.2018.65.3.335>

- Djilali N, Bousahla AA, Kaci A, Selim MM, Bourada F, Tounsi A, Tounsi A, Benrahou KH and Mahmoud SR (2022), “Large Cylindrical Deflection Analysis of FG Carbon Nanotube-Reinforced Plates in Thermal Environment Using a Simple Integral HSDT,” *Steel and Composite Structures*, **42**(6): 779–789. <https://doi.org/10.12989/SCS.2022.42.6.779>
- Dorafshan S, Behnamfar F, Khamesipour A and Motosaka M (2013), “Condensed Hyperelements Method of Non-Vertical Consistent Boundaries for Wave Propagation Analysis in Irregular Media,” *Earthquake Engineering and Engineering Vibration*, **12**(4): 547–559. <https://doi.org/10.1007/s11803-013-0196-7>
- Ebrahimi F and Seyfi A (2022), “Studying Propagation of Wave of Metal Foam Rectangular Plates with Graded Porosities Resting on Kerr Substrate in Thermal Environment via Analytical Method,” *Waves in Random and Complex Media*, **32**(2): 832–855. <https://doi.org/10.1080/17455030.2020.1802531>
- Ellali M, Amara K, Bouazza M and Bourada F (2018), “The Buckling of Piezoelectric Plates on Pasternak Elastic Foundation Using Higher-Order Shear Deformation Plate Theories,” *Smart Structures and Systems*, **21**(1): 113–122. <https://doi.org/10.12989/SSS.2018.21.1.113>
- Ellali M, Bouazza M and Amara K (2022a), “Thermal Buckling of a Sandwich Beam Attached with Piezoelectric Layers via the Shear Deformation Theory,” *Archive and Applied Mechanics*, **92**: 657–665. <https://doi.org/10.1007/s00419-021-02094-x>
- Ellali M, Bouazza M and Zenkour AM (2022b), “Impact of Micromechanical Approaches on Wave Propagation of FG Plates via Indeterminate Integral Variables with a Hyperbolic Secant Shear Model,” *International Journal of Computational Methods*, **19**(9): 2250019. <https://doi.org/10.1142/S0219876222500190>
- Ellali M, Bouazza M and Zenkour AM (2023), “Wave Propagation in Functionally-Graded Nanoplates Embedded in a Winkler-Pasternak Foundation with Initial Stress Effect,” *Physical Mesomechanics*, **26**: 282–294. <https://doi.org/10.1134/S1029959923030049>
- Ellali M, Bouazza M and Zenkour AM (2024a), “Hygrothermal Vibration of FG Nanobeam via Nonlocal Unknown Integral Variables Secant-Tangential Shear Deformation Coupled Theory with Temperature-Dependent Material Properties,” *European Journal of Mechanics-A/Solids*, **105**: 105243. <https://doi.org/10.1016/j.euromechsol.2024.105243>
- Ellali M, Zenkour AM, Bouazza M and Benseddiq N (2024b), “Thermal Buckling of FG Nanobeams via an Indeterminate Integral Variable with Trigonometric Displacement Models in Conjunction with the Gradient Elasticity Theory,” *Journal of Nano Research*, **82**: 117–138. <https://doi.org/10.4028/p-PCOnh6>
- Farrokhian A (2020), “The Effect of Voltage and Nanoparticles on the Vibration of Sandwich Nanocomposite Smart Plates,” *Steel and Composite Structures*, **34**(5): 733–742. <https://doi.org/10.12989/scs.2020.34.5.733>
- Farrokhian A and Salmani-Tehrani M (2020), “Surface and Small Scale Effects on the Dynamic Buckling of Carbon Nanotubes with Smart Layers Assuming Structural Damping,” *Steel and Composite Structures*, **37**(2): 229–251. <https://doi.org/10.12989/SCS.2020.37.2.229>
- Gafoura Y, Zidour M, Tounsi A, Heireche H and Semmah A (2013), “Sound Wave Propagation in Zigzag Double-Walled Carbon Nanotubes Embedded in an Elastic Medium Using Nonlocal Elasticity Theory,” *Physica E: Low-Dimensional Systems and Nanostructures*, **48**: 118–123. <https://doi.org/10.1016/j.physe.2012.11.006>
- Ghorbanpour Arani A, Haghparast E and Ghorbanpour Arani AH (2016a), “Size-Dependent Vibration of Double-Bonded Carbon Nanotube-Reinforced Composite Microtubes Conveying Fluid Under Longitudinal Magnetic Field,” *Polymer Composites*, **37**(5): 1375–1383. <https://doi.org/10.1002/pc.23306>
- Ghorbanpour Arani A, Jamali M, Ghorbanpour Arani AH, Kolahchi R and Mosayyebi M (2017a), “Electro-Magneto Wave Propagation Analysis of Viscoelastic Sandwich Nanoplates Considering Surface Effects,” *Proceedings of the Institution of Mechanical Engineers, Part C: Journal of Mechanical Engineering Science*, **231**(2): 387–403. <https://doi.org/10.1177/0954406215627830>
- Ghorbanpour Arani A, Jamali M, Mosayyebi M and Kolahchi R (2017b), “Analytical Modeling of Wave Propagation in Viscoelastic Functionally Graded Carbon Nanotubes Reinforced Piezoelectric Microplate Under Electro-Magnetic Field,” *Proceedings of the Institution of Mechanical Engineers, Part N: Journal of Nanomaterials, Nanoengineering and Nanosystems*, **231**(1): 17–33.
- Ghorbanpour Arani AH, Abdollahian M and Ghorbanpour Arani A (2020), “Nonlinear Dynamic Analysis of Temperature-Dependent Functionally Graded Magnetostrictive Sandwich Nanobeams Using Different Beam Theories,” *Journal of the Brazilian Society of Mechanical Sciences and Engineering*, **42**: No. 314. <https://doi.org/10.1007/s40430-020-02400-8>
- Ghorbanpour Arani AH, Rastgoo A, Hafizi Bidgoli A, Kolahchi R and Ghorbanpour Arani R (2017c), “Wave Propagation of Coupled Double-DWBNTs Conveying Fluid-Systems Using Different Nonlocal Surface Piezoelectricity Theories,” *Mechanics of Advanced Materials and Structures*, **24**(14): 1159–1179. <https://doi.org/10.1080/15376494.2016.1227488>
- Ghorbanpour Arani AH, Rastgoo A, Sharafi MM, Kolahchi R and Ghorbanpour Arani A (2016b), “Nonlocal Viscoelasticity Based Vibration of Double Viscoelastic Piezoelectric Nanobeam systems,” *Meccanica*, **51**: 25–40. <https://doi.org/10.1007/s11012-014-9991-0>
- Gong MS, Zuo ZX, Sun J, He RT and Zhao YN (2021), “Influence of the Column-to-Beam Flexural

- Strength Ratio on the Failure Mode of Beam-Column Connections in RC Frames,” *Earthquake Engineering and Engineering Vibration*, **20**(2): 441–452. <https://doi.org/10.1007/s11803-021-2030-y>
- Guo L, Xin XY, Shahsavari D and Karami B (2022), “Dynamic Response of Porous E-FGM Thick Microplate Resting on Elastic Foundation Subjected to Moving Load with Acceleration,” *Thin-Walled Structures*, **173**: 108981. <https://doi.org/10.1016/j.tws.2022.108981>
- Hachemi H, Bousahla AA, Kaci A, Bourada F, Tounsi A, Benrahou KH, Tounsi A, Al-Zahrani MM and Mahmoud SR (2021), “Bending Analysis of Functionally Graded Plates Using a New Refined Quasi-3D Shear Deformation Theory and the Concept of the Neutral Surface Position,” *Steel and Composite Structures*, **39**(1): 51–64. <http://doi.org/10.12989/scs.2021.39.1.051>
- Hadji M, Bouhadra A, Mamen B, Menasria A, Bousahla A, Bourada F, Bourada M, Benrahou KH and Tounsi A (2023), “Combined Influence of Porosity and Elastic Foundation Parameters on the Bending Behavior of Advanced Sandwich Structures,” *Steel and Composite Structures*, **46**(1): 1–13. <https://doi.org/10.12989/scs.2023.46.1.001>
- Hajmohammad MH, Farrokhan A and Kolahchi R (2021), “Dynamic Analysis in Beam Element of Wave-Piercing Catamarans Undergoing Slamming Load Based on Mathematical Modelling,” *Ocean Engineering*, **234**: 109269. <https://doi.org/10.1016/j.oceaneng.2021.109269>
- Hajmohammad MH, Maleki M and Kolahchi R (2018), “Seismic Response of Underwater Concrete Pipes Conveying Fluid Covered with Nano-Fiber Reinforced Polymer Layer,” *Soil Dynamics and Earthquake Engineering*, **110**: 18–27. <https://doi.org/10.1016/j.soildyn.2018.04.002>
- Hebali H, Chikh A, Bousahla AA, Bourada F, Tounsi A, Benrahou KH, Hussain M and Tounsi A (2022), “Effect of the Variable Visco-Pasternak Foundations on the Bending and Dynamic Behaviors of FG Plates Using Integral HSDT Model,” *Geomechanics and Engineering*, **28**(1): 49–64. <https://doi.org/10.12989/gae.2022.28.1.049>
- Hei BP, Yang ZL and Chen ZG (2016), “Scattering of Shear Waves by an Elliptical Cavity in a Radially Inhomogeneous Isotropic Medium,” *Earthquake Engineering and Engineering Vibration*, **15**(1): 145–151. <https://doi.org/10.1007/s11803-016-0311-7>
- Heidari E and Ariaei A (2022), “A New Approach for Free Vibration Analysis of a System of Elastically Interconnected Similar Rectangular Plates,” *Earthquake Engineering and Engineering Vibration*, **21**(4): 947–967. <https://doi.org/10.1007/s11803-022-2129-9>
- Hentati H, Kriaa Y, Haugou G, Chaari F, Wali M, Zouari B and Dammak F (2017), “Influence of Elastic Wave on Crack Nucleation – Experimental and Computational Investigation of Brittle Fracture,” *Applied Acoustics*, **128**: 45–54.
- Karami B, Shahsavari D and Li L (2018) “Temperature-Dependent Flexural Wave Propagation in Nanoplate-Type Porous Heterogenous Material Subjected to In-Plane Magnetic Field,” *Journal of Thermal Stresses*, **41**(4): 483–499. <https://doi.org/10.1080/01495739.2017.1393781>
- Keshtegar B, Farrokhan A, Kolahchi R and Trung NT (2020a), “Dynamic Stability Response of Truncated Nanocomposite Conical Shell with Magnetostrictive Face Sheets Utilizing Higher Order Theory of Sandwich Panels,” *European Journal of Mechanics-A/Solids*, **82**: 104010. <https://doi.org/10.1016/j.euromechsol.2020.104010>
- Keshtegar B, Motezaker M, Kolahchi R and Trung NT (2020b), “Wave Propagation and Vibration Responses in Porous Smart Nanocomposite Sandwich Beam Resting on Kerr Foundation Considering Structural Damping,” *Thin-Walled Structures*, **154**: 106820. <https://doi.org/10.1016/j.tws.2020.106820>
- Kolahchi R, Keshtegar B and Trung NT (2022), “Optimization of Dynamic Properties for Laminated Multiphase Nanocomposite Sandwich Conical Shell in Thermal and Magnetic Conditions,” *Journal of Sandwich Structures & Materials*, **24**(1): 643–662. <https://doi.org/10.1177/10996362211020388>
- Kolahchi R, Zhu SP, Keshtegar B and Trung NT (2020), “Dynamic Buckling Optimization of Laminated Aircraft Conical Shells with Hybrid Nanocomposite Material,” *Aerospace Science and Technology*, **98**: 105656. <https://doi.org/10.1016/j.ast.2019.105656>
- Kouider D, Kaci A, Selim MM, Bousahla AA, Bourada F, Tounsi A, Tounsi A and Hussain M (2021), “An Original Four-Variable Quasi-3D Shear Deformation Theory for the Static and Free Vibration Analysis of New Type of Sandwich Plates with Both FG Face Sheets and FGM Hard Core,” *Steel and Composite Structures*, **41**(2): 167–191. <https://doi.org/10.12989/SCS.2021.41.2.167>
- Li L, Hu YJ and Ling L (2015), “Flexural Wave Propagation in Small-Scaled Functionally Graded Beams via a Nonlocal Strain Gradient Theory,” *Composite Structures*, **133**: 1079–1092. <https://doi.org/10.1016/j.compstruct.2015.08.014>
- Li L, Li XB and Hu YJ (2016), “Free Vibration Analysis of Nonlocal Strain Gradient Beams Made of Functionally Graded Material,” *International Journal of Engineering Science*, **102**: 77–92. <https://doi.org/10.1016/j.ijengsci.2016.02.010>
- Liang Y, Zhao FL, Luo J and Chen P (2022), “Study on Time-Varying Seismic Vulnerability and Analysis of ECC-RC Composite Piers Using High Strength Reinforcement Bars in Offshore Environment,” *Earthquake Engineering and Engineering Vibration*, **21**(4): 1035–1051. <https://doi.org/10.1007/s11803-022-2123-2>
- Liu GL, Wu SB, Shahsavari D, Karami B and Tounsi A (2022), “Dynamics of Imperfect Inhomogeneous Nanoplate with Exponentially-Varying Properties

- Resting on Viscoelastic Foundation,” *European Journal of Mechanics-A/Solids*, **95**: 104649. <https://doi.org/10.1016/j.euromechsol.2022.104649>
- Luo C, Lou ML, Gui GQ and Wang H (2019), “A Modified Domain Reduction Method for Numerical Simulation of Wave Propagation in Localized Regions,” *Earthquake Engineering and Engineering Vibration*, **18**(1): 35–52. <https://doi.org/10.1007/s11803-019-0488-7>
- Merazka B, Bouhadra A, Menasria A, Selim MM, Bousahla AA, Bourada F, Tounsi A, Benrahou KH, Tounsi A, Al-Zahrani MM (2021), “Hygro-Thermo-Mechanical Bending Response of FG Plates Resting on Elastic Foundations,” *Steel and Composite Structures*, **39**(5): 631–643. <https://doi.org/10.12989/scs.2021.39.5.631>
- Mudhaffar IM, Tounsi A, Chikh A, Al-Osta MA, Al-Zahrani MM and Al-Dulaija SU (2021), “Hygro-Thermo-Mechanical Bending Behavior of Advanced Functionally Graded Ceramic Metal Plate Resting on a Viscoelastic Foundation,” *Structures*, **33**: 2177–2189. <https://doi.org/10.1016/j.istruc.2021.05.090>
- Nacéri M, Zidour M, Semmah A, Houari MSA, Benzair A and Tounsi A (2011), “Sound Wave Propagation in Armchair Single Walled Carbon Nanotubes Under Thermal Environment,” *Journal of Applied Physics*, **110**(12): 124322. <https://doi.org/10.1063/1.3671636>
- Nami MR and Janghorban M (2014), “Wave Propagation in Rectangular Nanoplates Based on Strain Gradient Theory with One Gradient Parameter with Considering Initial Stress,” *Modern Physics Letters B*, **28**(3): 1450021.
- Pitakthapanaphong S and Busso EP (2002), “Self-Consistent Elasto-Plastic Stress Solutions for Functionally Graded Material Systems Subjected to Thermal Transients,” *Journal of the Mechanics and Physics of Solids*, **50**(4): 695–716.
- Qian ZH, Jin F, Lu TJ and Kishimoto K (2009), “Transverse Surface Waves in an FGM Layered Structure,” *Acta Mechanica*, **207**: 183–193. <https://doi.org/10.1007/s00707-008-0123-6>
- Shahsavari D, Karami B and Li L (2018), “A High-Order Gradient Model for Wave Propagation Analysis of Porous FG Nanoplates,” *Steel and Composite Structures*, **29**(1): 53–66.
- Shahsavari D, Karami B and Tounsi A (2023), “Wave Propagation in a Porous Functionally Graded Curved Viscoelastic Nano-Size Beam,” *Waves in Random and Complex Media*, Online. <https://doi.org/10.1080/17455030.2022.2164376>
- Sun D and Luo SN (2011), “Wave Propagation of Functionally Graded Material Plates in Thermal Environments,” *Ultrasonics*, **51**(8): 940–952.
- Tahir SI, Chikh A, Tounsi A, Al-Osta MA, Al-Dulaijan SU and Al-Zahrani MM (2021a), “Wave Propagation Analysis of a Ceramic-Metal Functionally Graded Sandwich Plate with Different Porosity Distributions in a Hygro-Thermal Environment,” *Composite Structures*, **269**: 114030. <https://doi.org/10.1016/j.compstruct.2021.114030>
- Tahir SI, Tounsi A, Chikh A, Al-Osta MA, Al-Dulaijan SU and Al-Zahrani MM (2021b), “An Integral Four-Variable Hyperbolic HSDT for the Wave Propagation Investigation of a Ceramic-Metal FGM Plate with Various Porosity Distributions Resting on a Viscoelastic Foundation,” *Waves in Random and Complex Media*, Online. <https://doi.org/10.1080/17455030.2021.1942310>
- Tahir SI, Tounsi A, Chikh A, Al-Osta MA, Al-Dulaijan SU and Al-Zahrani MM (2022), “The Effect of Three-Variable Viscoelastic Foundation on the Wave Propagation in Functionally Graded Sandwich Plates via a Simple Quasi-3D HSDT,” *Steel and Composite Structures*, **42**(4): 501–511. <https://doi.org/10.12989/SCS.2022.42.4.501>
- Wan PH, Al-Furjan MSH, Kolahchi R and Shan L (2023), “Application of DQHFEM for Free and Forced Vibration, Energy Absorption, and Post-Buckling Analysis of a Hybrid Nanocomposite Viscoelastic Rhombic Plate Assuming CNTs’ Waviness and Agglomeration,” *Mechanical Systems and Signal Processing*, **189**: 110064. <https://doi.org/10.1016/j.ymssp.2022.110064>
- Wang JX, Li HJ and Xing HJ (2022), “A Lumped Mass Chebyshev Spectral Element Method and Its Application to Structural Dynamic Problems,” *Earthquake Engineering and Engineering Vibration*, **21**(3): 843–859. <https://doi.org/10.1007/s11803-022-2117-0>
- Wang Y, Yang ZL, Zhang JW and Yang Y (2017), “Theory and Application of Equivalent Transformation Relationships Between Plane Wave and Spherical Wave,” *Earthquake Engineering and Engineering Vibration*, **16**(4): 773–782. <https://doi.org/10.1007/s11803-017-0413-x>
- Wang YZ, Li FM and Kishimoto K (2010), “Scale Effects on Flexural Wave Propagation in Nanoplate Embedded in Elastic Matrix with Initial Stress,” *Applied Physics A*, **99**: 907–911.
- Xie MX, Hu YD and Xu HR (2023), “Simultaneous Resonance of an Axially Moving Ferromagnetic Thin Plate Under a Line Load in a Time-Varying Magnetic Field,” *Earthquake Engineering and Engineering Vibration*, **22**(4): 951–963. <https://doi.org/10.1007/s11803-023-2215-7>
- Yang ZL, Wang Y and Hei BP (2013), “Transient Analysis of 1D Inhomogeneous Media by Dynamic Inhomogeneous Finite Element Method,” *Earthquake Engineering and Engineering Vibration*, **12**(4): 569–576. <https://doi.org/10.1007/s11803-013-0198-5>
- Yang ZY, Xie Q, He C and Xue ST (2021), “Numerical Investigation of the Seismic Response of a UHV Composite Bypass Switch Retrofitted with Wire Rope Isolators,” *Earthquake Engineering and Engineering Vibration*, **20**(1): 275–290. <https://doi.org/10.1007/s11803-021-2019-6>

- Zaitoun MW, Chikh A, Tounsi A, Al-Osta MA, Sharif A, Al-Dulaijan SU and Al-Zahrani MM (2022), "Influence of the Visco-Pasternak Foundation Parameters on the Buckling Behavior of a Sandwich Functional Graded Ceramic-Metal Plate in a Hygrothermal Environment," *Thin-Walled Structures*, **170**: 108549. <https://doi.org/10.1016/j.tws.2021.108549>
- Zeng XZ, Zhu SC, Deng KL, Zhao CH and Zhou YY (2023), "Experimental and Numerical Study on Cyclic Behavior of A UHPC-RC Composite Pier," *Earthquake Engineering and Engineering Vibration*, **22**(3): 731–745. <https://doi.org/10.1007/s11803-023-2185-9>
- Zhang LW, Huang DM and Liew KM (2015), "An Element-Free IMLS-Ritz Method for Numerical Solution of Three-Dimensional Wave Equations," *Computer Methods in Applied Mechanics and Engineering*, **297**: 116–139. <https://doi.org/10.1016/j.cma.2015.08.018>
- Zhang WX, Lv WL, Zhang JY, Wang X, Hwang HJ and Yi WJ (2021), "Energy-Based Dynamic Parameter Identification for Pasternak Foundation Model," *Earthquake Engineering and Engineering Vibration*, **20**(3): 631–643. <https://doi.org/10.1007/s11803-021-2043-6>
- Zhang XM, Li Z and Yu JG (2018), "Evanescence Waves in FGM Spherical Curved Plates: An Analytical Treatment," *Meccanica*, **53**: 2145–2160. <https://doi.org/10.1007/s11012-017-0800-4>
- Zhang YT, Jiang LZ, Zhou WB, Liu SH, Feng YL, Liu X and Lai ZP (2022), "Dynamic Response Analysis of a Multiple-Beam Structure Subjected to a Moving Load," *Earthquake Engineering and Engineering Vibration*, **21**(3): 769–784. <https://doi.org/10.1007/s11803-022-2106-3>